eJSSNT ALC '19 Conference

e-Journal of Surface Science and Nanotechnology **18**, 24–27 (2020)

Active Phase Structure of the SiO_2-supported Nickel Phosphide Catalysts for Non-oxidative Coupling of Methane (NOCM) Reactions

M. H. Al Rashid,[a] A. Dipu,[b] Y. Nishikawa,[b] H. Ogihara,[c] Y. Inami,[b] S. Obuchi,[b] I. Yamanaka,[b] S. Nagamatsu,[d] D. Kido,[a] K. Asakura [d, †]

[a] *Graduate School of Engineering, Hokkaido University, Sapporo 060-8628, Hokkaido, Japan*
[b] *Department of Chemistry and Material Science, Tokyo Institute of Technology, Tokyo 152-8551, Japan*
[c] *Graduate School of Science and Engineering, Saitama University, Saitama 338-8570, Japan*
[d] *Institute for Catalysis, Hokkaido University, Hokkaido 001-0021, Japan*
[†] *Corresponding author: askr@cat.hokudai.ac.jp*

Received: 21 October, 2019, Accepted 30 January, 2020, Published 15 February, 2020

SiO_2-supported NiP binary catalysts show high activity for the non-oxidative coupling of methane (NOCM) reactions, one of the most difficult but important catalytic reactions. We have studied the SiO_2-supported NiP binary catalysts by extended X-ray absorption fine structure (EXAFS) with different Ni : P ratios. NiP binary catalyst with the composition of Ni : P = 1 : 1 was the most active among the three different compositions. EXAFS showed that the NiP catalyst with Ni : P = 1 : 1 had a Ni_2P structure. The structure was stable after the high temperature (1173 K) NOCM reaction conditions for 12 h. It is interesting that Ni_2P shows high catalytic activities in many other reactions such as hydrodesulfurization, hydrogen evolution reaction, and so on. It may be due to the appropriate electronic and geometrical modification of a Ni active site by P.

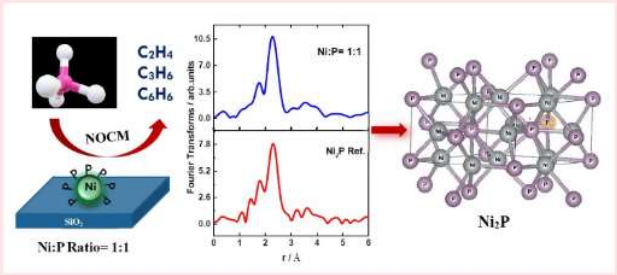

Keywords *EXAFS; Nickel phosphide; Ni_2P; Non-oxidative coupling of methane*

I. INTRODUCTION

Extended X-ray absorption fine structure (EXAFS) spectroscopy is the most promising technique used for the atomic-level characterization of the inorganic-oxide-supported catalysts. Recently, due to the oil depletion of petroleum, many attentions have been paid to the utilization of CH_4 for organic material feedstock syntheses. One way to convert methane to the higher hydrocarbons is non-oxidative coupling of methane (NOCM) reactions using catalysts at high temperature.

Recently, Yamanaka *et al.* screened catalytic activities of various Ni-M/SiO_2 compounds (M = metals or metalloids) for the NOCM reactions using a fixed bed-gas-flow system at 1173 K and found that SiO_2-supported NiP catalysts showed highest activity for the NOCM reaction to produce hydrocarbons at 1173 K among the others [1]. There was a strong dependence on the ratio of Ni : P, and Ni : P = 1 : 1 showed the best performance as shown in Figure S1 in Supplementary Material. Figure S2 (Supplementary Material) shows the X-ray diffraction (XRD) result. Ni : P = 1 : 1 gave the peaks corresponding to Ni_2P crystalline. The crystalline size was 30–40 nm from the peak width. However, XRD was not so sensitive to the structures of nanoparticles or amorphous phases.

In this research, we applied EXAFS to elucidate the active structure of NiP catalysts with different Ni : P ratios before and after NOCM reactions.

II. EXPERIMENTAL

The SiO_2-supported NiP catalysts with initial NiP ratios of

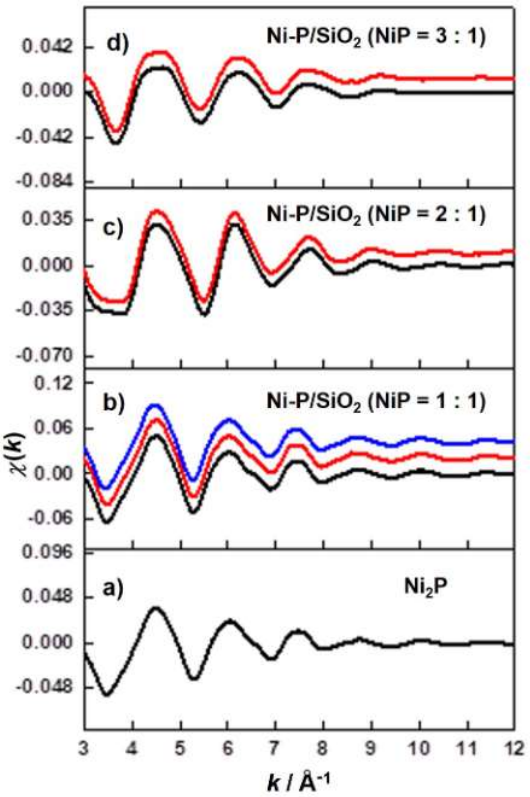

Figure 1: Comparison of EXAFS; (a) reference Ni_2P, (b) Ni-P/SiO_2 (Ni : P = 1 : 1), (c) Ni-P/SiO_2 (Ni : P = 2 : 1), and (d) Ni-P/SiO_2 (Ni : P = 3 : 1). The reaction times for the Ni-P/SiO_2 samples are 0 h (black), 3 h (red), and 12 h (blue).

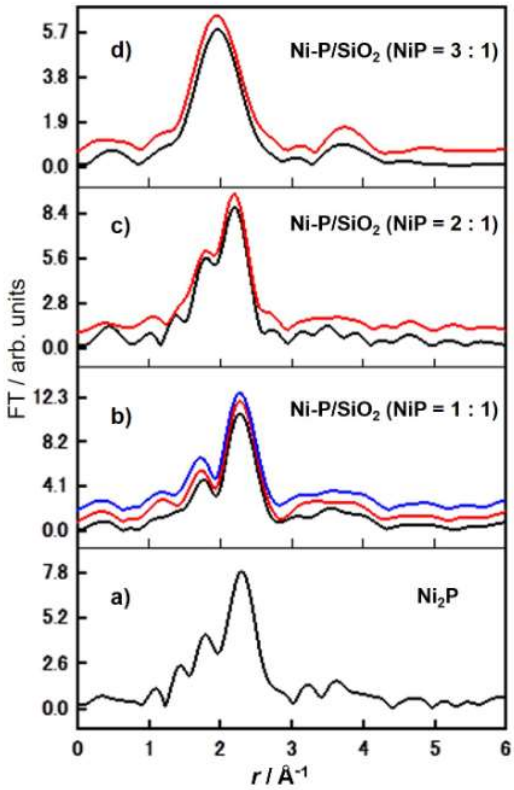

Figure 2: Comparison of Fourier transforms; (a) reference Ni_2P, (b) Ni-P/SiO_2 (Ni : P = 1 : 1), (c) Ni-P/SiO_2 (Ni : P = 2 : 1), and (d) Ni-P/SiO_2 (Ni : P = 3 : 1). The reaction times for the Ni-P/SiO_2 samples are 0 h (black), 3 h (red), and 12 h (blue).

1 : 1, 2 : 1, and 3 : 1 were prepared by a conventional impregnation method, followed by temperature programmed reduction. The preparation details can be found in the Supporting Information of Ref. 1. The sample was denoted as Ni-P/SiO_2 (NiP = X : Y, Z h) where X : Y represents the Ni : P ratio and Z is the reaction time. Before performing each NOCM reaction, the catalyst was purged by 10 mL min^{-1} of Ar while the temperature increased from room temperature to 1173 K at a rate of 25 K min^{-1}. Pure methane was flowed at 10 mL min^{-1} into the reactor at 1173 K.

EXAFS measurements were carried out at BL9C of the Photon Factory (PF) in Institute for Structure Materials Science, High Energy Accelerator Research Organization (KEK) operated at 2.5 GeV, 450 mA. The emitted X-ray was monochromatized by a Si (111) double crystal and focused with a Rh coated bent cylindrical mirror. The EXAFS analyses were carried out by the REX2000 (Rigaku Co.) [2]. The theoretical amplitude and phase shift functions of Ni–Ni and Ni–P atom-pairs were calculated by FEFF8 [3]. The two- shell fitting for Ni–Ni and Ni–P bonds provided the bond distances, coordination numbers, and the other structure parameters. The number of fitting parameters was less than the values determined by the formula, $N_{ind} = 2\Delta k\Delta R/\pi + 2$ [4], where N_{ind} is a number of independent parameters, Δk is a range of used data in the wave number k, and ΔR is a range of used data in the interatomic distance R.

III. RESULTS AND DISCUSSION

Figure 1 shows the EXAFS oscillations [an EXAFS oscillation, $\chi(k)$, vs. the photoelectron wave number, k] of the fresh and spent samples with different initial Ni : P ratios after background subtraction. The three different Ni : P ratio samples give different oscillations. Figure 1(b) shows the EXAFS oscillation of the sample Ni-P/SiO_2 (Ni : P = 1 : 1, 0 h), which was similar to that of the Ni_2P reference as shown in Figure 1(a), indicating that Ni-P/SiO_2 (Ni : P = 1 : 1, 0 h) had mostly the Ni_2P structure. Ni-P/SiO_2 (Ni : P = 2 : 1, 0 h) and Ni-P/SiO_2 (Ni : P = 3 : 1, 0 h) had quite different oscillations from those of Ni_2P reference as shown in Figure 1(c, d). We could not find little change in the spent samples with various Ni : P ratios even after the high temperature reactions at 1173 K. The NiP catalysts had high stability.

Figure 2 shows the Fourier transforms of the Ni K-edge EXAFS spectra for the fresh and spent samples. The Ni-P /SiO_2 (Ni : P = 1 : 1, 0 h) showed two distinct peaks in this Fourier transform as shown in Figure 2(b). The first and main peak were corresponding to the Ni–P and Ni–Ni

Table 1: Curve fitting results of the Ni K-edge EXAFS spectra for the Ni_2P reference and different samples with initial Ni : P ratios of 1 : 1, 2 : 1, and 3 : 1.

Samples	Ni-Ni				Ni-P				R%[e]
	CN[a]	R (Å)[b]	σ(Å)[c]	ΔE (eV)[d]	CN[a]	R (Å)[b]	σ(Å)[c]	ΔE (eV)[d]	
				Fresh samples					
Ni_2P reference	4.0±0.3	2.62±0.02	0.092	5.4	1.0±0.3	2.21±0.02	0.071	-5.1	0.5
Ni-P (1:1, 0h)	4.6±0.6	2.62±0.02	0.085	3.4	1.3±0.3	2.19±0.02	0.081	-7.5	0.3
Ni-P (2:1, 0h)	4.2±0.3	2.52±0.02	0.093	-1.1	0.6±0.3	2.18±0.03	0.036	-7.3	0.1
Ni-P (3:1, 0h)	4.6±0.9	2.45±0.02	0.116	-7.2	2.0±0.5	2.28±0.02	0.139	-3.6	0.5
				Spent samples					
Ni-P (1:1, 3h)	4.5±0.8	2.62±0.03	0.082	3.5	1.5±0.5	2.18±0.03	0.084	-9.8	0.5
Ni-P (2:1, 3h)	4.3±0.3	2.53±0.03	0.095	-0.7	0.7±0.3	2.17±0.03	0.058	-8.8	0.3
Ni-P (3:1, 3h)	4.6±1.0	2.46±0.02	0.117	-6.6	2.1±0.6	2.28±0.03	0.131	-2.3	0.4

[a] Coordination number.
[b] Interatomic distance.
[c] σ ; Debye-Waller factor.
[c] Edge shift.
[e] Residual factor.

distances, respectively. Compared to the reference compound, the Fourier transform depicted the similar pattern to that of Ni_2P as shown in Figure 2(a). The curve fitting analyses indicated the Ni–P and Ni–Ni distances were 2.19 Å and 2.62 Å, respectively, as shown in Table 1. These bond lengths agree well with those found in Ni_2P reference within the error bar. We concluded that the N_2P structure was only found in the sample Ni-P/SiO_2 (Ni : P = 1 : 1, 0 h). With increase of the Ni : P ratio, the main peak corresponding to Ni–Ni was shifted towards the shorter bond distance. Ni-P/SiO_2 (Ni : P = 1 : 1, 0 h) sample showed the smaller peak intensity in the main peak as shown in Figure 2(c). Curve fitting analyses indicated the Ni–Ni bond distance was 2.52 Å while that of Ni–P was 2.18 Å. The Ni–P bond distances in Ni-P/SiO_2 (Ni : P = 1 : 1, 0 h) and Ni-P/SiO_2 (Ni : P = 2 : 1, 0 h) were almost the same. In the case of NiP (3 : 1, 0 h), the two peaks were merged into one and a broad peak appeared at a shorter bond distance as shown in Figure 2(d). The curve fitting analyses showed the Ni–P and Ni–Ni distances were 2.28 Å and 2.45 Å, respectively. The Ni–Ni distance was shorter than that of Ni metal (2.48 Å) as shown in Table 1.

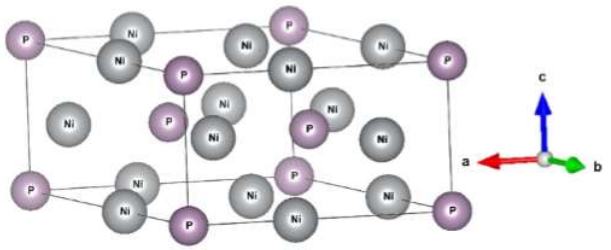

Figure 3: Bulk structure of Ni_2P. Ni_2P consists of two consecutive plane Ni_3P_2 and Ni_3P.

We could characterize the most active Ni-P/SiO_2 (Ni : P = 1 : 1) catalyst as Ni_2P successfully, which was consistent with X-ray diffraction analysis as shown in Figure S2 (Supplementary Material). It is difficult to derive the structures about the NiP (2 : 1, 0 h) and NiP (3 : 1, 0 h) only from EXAFS because of less informative features of EXAFS oscillations. But we could say that there is no indication of the formation of Ni metal nanoclusters, because we always found the Ni–Ni distance for NiP (2 : 1, 0 h) or NiP (3 : 1, 0 h) was longer or shorter than that of Ni metal as shown in Table 1, respectively. We are now carrying out the XANES (X-ray absorption near edge structure) analysis using these possible crystalline structures.

Recently Ni_2P catalysts draw many attentions. It shows a high catalytic activity in hydrogen related reactions, such as hydrodesulfurization reactions [5, 6], hydrodeoxidation [7, 8], and hydrogen evolution reactions [9, 10], Ni_2P has a crystal structure as shown in Figure 3 [11]. Along the c axis, two-layer structures are alternatively stacked. One is called as Ni_3P and the other is Ni_3P_2. Scanning tunneling microscopy (STM) and low energy electron diffraction (LEED) of the Ni_2P single crystal showed Ni_3P_2 was mainly present on the Ni_2P(0001) surface [12–16].

Both Ni_3P and Ni_3P_2 structures have three-fold Ni hollow sites surrounded by P. The three-fold Ni hollow sites might be the active site and P should modify the electronic structure of Ni as well as the isolation of too much active Ni hollow sites [12]. This might prohibit undesired coke formations and more selectively cleave the C–H bond. Moreover, the isolation of Ni sites might slow down the chain expansion reaction and C_2H_4 formation becomes preferable.

We used more P than stoichiometry to have a Ni_2P structure. In the previous studies, the NiP ratio of 1 : 1 was required to prepare the Ni_2P structure [17], because we

found that the evaporation of P at high temperature under reductive or ultrahigh vacuum conditions [18]. Less P induces the phase transition to $Ni_{12}P_5$ or the other phase. The extra PO_4 species present on the surface might play the role of the P supplier. Thus, Ni : P = 1 : 1 gives the Ni_2P structure stably.

Above discussion is based on the assumption that the surface structure is the same as the bulk terminated and the structure under the working conditions is identical to that before and after the reaction. In order to reveal the real active site structure, we are going to carry out *in situ* EXAFS measurements of Ni_2P catalysts at 1173 K under the flow of methane like the EXAFS analysis of In/SiO_2 NOCM catalyst [19].

IV. CONCLUSIONS

We investigated the structure of active NiP binary catalysts by EXAFS. The most active catalyst had Ni_2P structure and its structure was stable during non-oxidative coupling of methane (NOCM) reactions at 1173 K. P might control the Ni activity not to form the C–C bond by geometrically or electronically.

Acknowledgments

We performed these experiments under the CREST project "Innovative Catalysts" JPMJCR15P4 of Japan Science and Technology (JST). All the XAFS work was performed at KEK-PF under proposal numbers 2016G546 and 2018G628. We thanks to all XAFS team members in Photon Factory for their technical supports.

Appendix

Details of catalysts preparation, dependence of yield of hydrocarbons on the Ni : P ratios, and catalyst characterizations other than EXAFS are available in Supplementary Material at https://doi.org/10.1380/ejssnt.2020.24.

Note

This paper was presented at the 12th International Symposium on Atomic Level Characterizations for New Materials and Devices '19 (ALC '19), in conjunction with the 22nd International Conference on Secondary Ion Mass Spectrometry (SIMS-22), Miyako Messe, Kyoto, Japan, 20–25 October, 2019.

References

[1] A. L. Dipu, S. Ohbuchi, Y. Nishikawa, S. Iguchi, H. Ogihara, and I. Yamanaka, ACS Catal. **10**, 375 (2020).
[2] K. Asakura, in: *X-Ray Absorption Fine Structure for Catalysts and Surfaces*, edited by Y. Iwasawa (World Scientific, Singapore, 1996) pp. 33–58.
[3] S. I. Zabinsky, J. J. Rehr, A. Ankudinov, R. C. Albers, and M. J. Eller, Phys. Rev. B **52**, 2995 (1995).
[4] E. A. Stern, Phys. Rev. B **48**, 9825 (1993).
[5] S. T. Oyama, T. Gott, H. Zhao, and Y.-K. Lee, Catal. Today **143**, 94 (2009).
[6] J. A. Rodriguez, J.-Y. Kim, J. C. Hanson, S. J. Sawhill, and M. E. Bussell, J. Phys. Chem. B **107**, 6276 (2003).
[7] Y. Yang, C. Ochoa-Hernández, V. A. de la Peña O'Shea, J. M. Coronado, and D. P. Serrano, ACS Catal. **2**, 592 (2012).
[8] A. Iino, A. Takagaki, R. Kikuchi, S. T. Oyama, and K. K. Bando, J. Phys. Chem. C **123**, 7633 (2019).
[9] J.-S. Moon, J.-H. Jang, E.-G. Kim, Y.-H. Chung, S. J. Yoo, and Y.-K. Lee, J. Catal. **326**, 92 (2015).
[10] L. Feng, H. Vrubel, M. Bensimon, and X. Hu, Phys. Chem. Chem. Phys. **16**, 5917 (2014).
[11] S. Rundqvist, Acta Chem. Scand. **16**, 992 (1962).
[12] M. G. Moula, S. Suzuki, W. J. Chun, S. Otani, S. T. Oyama, and K. Asakura, Chem. Lett. **35**, 90 (2006).
[13] A. B. Hernandez, H. Ariga, S. Takakusagi, K. Kinoshita, S. Suzuki, S. Otani, S. T. Oyama, and K. Asakura, Chem. Phys. Lett. **513**, 48 (2011).
[14] H. Ariga, M. Kawashima, S. Takakusagi, and K. Asakura, Chem. Lett. **42**, 1481 (2013).
[15] Q. Yuan, H. Ariga, and K. Asakura, Top. Catal. **58**, 194 (2015).
[16] P. Liu and J. A. Rodriguez, J. Am. Chem. Soc. **127**, 14871 (2005).
[17] S. T. Oyama, X. Wang, Y.-K. Lee, K. Bando, and F. G. Requejo, J. Catal. **210**, 207 (2002).
[18] T. Miyamoto, *The Study for Revealing the Origins of the Properties of Advanced Functional Materials Using Quantum Beams*, Ph.D. Thesis, Hokkaido University, 2010.
[19] U. Kashaboina, Y. Nishikawa, Y. Wakisaka, N. Sirisit, S. Nagamatsu, D. Bao, H. Ariga-Miwa, S. Takakusagi, Y. Inami, F. Kuriyama, A. L. Dipu, H. Ogihara, S. Iguchi, I. Yamanaka, T. Wada, and K. Asakura, Chem. Lett. **48**, 1145 (2019).